

Structural, optical and magnetic properties of Ni-doped CdS thin films prepared by CBD

R. Premarani · J. Jebaraj Devadasan ·
S. Saravanakumar · R. Chandramohan ·
T. Mahalingam

Received: 3 September 2014 / Accepted: 22 December 2014 / Published online: 30 December 2014
© Springer Science+Business Media New York 2014

Abstract Room-temperature ferromagnetic behavior of undoped cadmium sulphide (CdS) and Ni-doped CdS thinfilms prepared by chemical bath deposition technique is reported. The crystallite sizes of the thinfilms have been characterized by X-ray diffraction pattern. The particle sizes increase from 11 to 40 nm with the increase of Ni content in the CdS thinfilms. scanning electron microscope results indicated that CdS thinfilms is made up of aggregate of spherical-like particles. The composition was estimated by Energy dispersive analysis of X-ray and reported. Spectroscopic studies revealed considerable improvement in transmission and the band gap of the films decreased from 2.62 to 2.28 eV with addition of Ni dopant that is associated with variation in crystallite sizes in the nano regime. Magnetization measurements indicate that the Ni doped CdS thinfilms exhibited ferromagnetism and the saturation magnetization decreases with the increase of crystal sizes in the Ni doped CdS nano thinfilms. This finding in CdS thinfilms should be focus of the future electronic and spintronics devices.

R. Premarani
Department of Physics, Arumugam Pillai Seethai Ammal
College, Thiruppattur, Tamilnadu, India

J. Jebaraj Devadasan
Research Department of Physics, Pope's College, Sawyerpuram,
Tamilnadu, India

S. Saravanakumar · R. Chandramohan (✉)
PG and Research Department of Physics, Sree Sevugan
Annamalai College, Devakottai, Tamilnadu, India
e-mail: rathinam.chandramohan@gmail.com

T. Mahalingam
Department of Electrical and Computer Engineering,
Ajou University, Suwon 443-749, South Korea

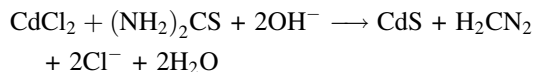
1 Introduction

In recent studies, nanometer scale materials much interest because it exhibits new or enhanced size dependent properties compared with the larger size particles of the same material [1]. Nano semiconductor materials exhibit host of mechanical, electrical, and optical properties, which are superior to those of the individual components [2, 3]. CdS is the direct band gap II–VI semiconductor material having a bandgap 2.42 eV at room temperature. Transition metal (Mn, Ni, Cu etc.) doped CdS has drawn considerable attention as it affects the optical and luminescence properties. As recently II–VI semiconductor materials have much attention for room temperature ferromagnetism [4]. The RTFM in CdS has great development in the fabrication of magneto-optical and spintronics devices [5–8]. Deposition techniques such as sputtering [9], pulsed laser deposition [10], spray pyrolysis [11] and chemical bath deposition technique [12] have already been employed to prepare thin films. CdS and Ni doped CdS thin films were obtained through chemical bath deposition technique. Chemical bath deposition technique is simple, low cost and effective method for preparation of nano sized thin films [13]. In this study, we investigate the structural, optical and magnetic properties of undoped and Ni doped CdS thinfilms.

2 Experimental

The deposition of CdS thinfilms were carried out on sonicated cleaned glass substrate. For CBD, the composition of the bath was maintained with 7.5 ml of 0.2 M $\text{CdCl}_2 \cdot 2\text{H}_2\text{O}$, 10 ml of 0.1 M NH_4Cl , 7.5 ml of 0.5 M $\text{CS}(\text{NH}_2)_2$, 25 ml of 2 M NH_4OH and 10 ml of 0.6 mM

EDTA. For preparing of Ni doped films of various compositions, ratio of 0.2 M $\text{NiCl}_2 \cdot 5\text{H}_2\text{O}$ and $\text{CdCl}_2 \cdot 2\text{H}_2\text{O}$ is varied as per requirement. Deposition was carried out at the constant bath temperature of 80 °C. All the experiments were maintained for 60 min. The deposited films were dried in air and subsequently annealed at the temperature of 300 °C for an hour. All the films were dark yellow in color. The proposed overall mechanism for the deposition of CdS is



The structural properties the film were studied by X-ray diffractometer system (X'PERT Pro PANalytical, Netherlands) with $\text{CuK}\alpha$ radiation ($\lambda = 0.1540$ nm) by varying the diffraction angle 2θ with a step width of 0.02° . Surface morphological studies were carried out by scanning electron microscope (JEOL model JSM-6701F, Japan) and AFM-(Nano surf Easy scan 2) AGILENT-N9410A-5500 measurements in contact mode. Optical transmittance was measured by Perkin Elements Lambda 35 UV-Vis spectrometer. Magnetic properties of the films were studied with Vibrating Sample Magnetometer (VSM, Model; PAR 4500). The structural, optical and magnetic characterizations of $\text{Cd}_{1-x}\text{Ni}_x\text{S}$ were done the range of methods.

3 Results and discussions

The structural studies using XRD patterns obtained for undoped and Ni doped CdS nano thin films confirms that they exhibit cubic structure as per the standard JCPDS card no. 89-0440. The 2θ values of the diffraction peaks are

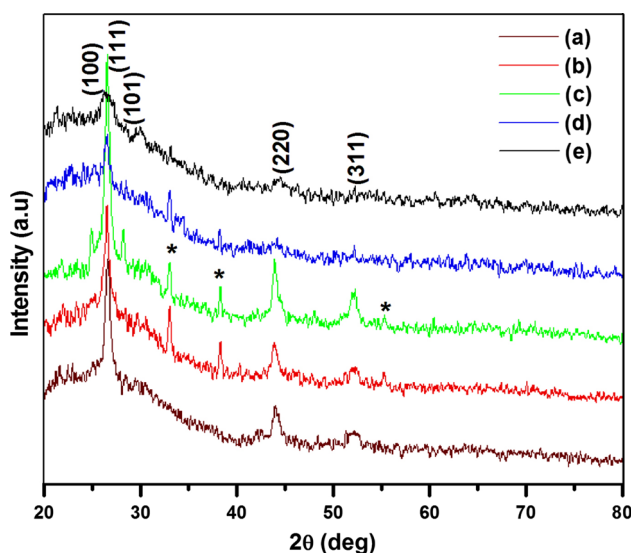


Fig. 1 X-ray diffraction pattern of $\text{Cd}_{1-x}\text{Ni}_x\text{S}$ thinfilms obtained at various Ni concentrations

observed at 26.46° , 43.89° and 51.97° respectively which corresponds to reflections from (111), (220) and (311) planes for undoped and Ni doped CdS thinfilms. With increasing Ni concentration, the peak (111) slightly shift to lower angle which indicates the increased lattice parameter in $\text{Cd}_{1-x}\text{Ni}_x\text{S}$ ($x = 0.06$ and 0.08) thinfilms. It may assign by the presence of dopant (Ni) contents (or) it was aroused due to the lattice contraction in nano structure Fig. 1.

The hexagonal phase based peaks (100) and (101) were identified in Ni doped CdS films. This indicates that Ni doping stabilizes hexagonal phase in CdS. But some extra Nickel Sulfide based peaks appeared in Ni doped CdS films which were indicated by asterisks (*). This Ni_2S lattice has affected the crystalline nature of CdS film. The shift in prominent peak towards lower angles is shown in Fig. 2 with increasing x . The average crystallite sizes are calculated using Debyes Scherrer formula

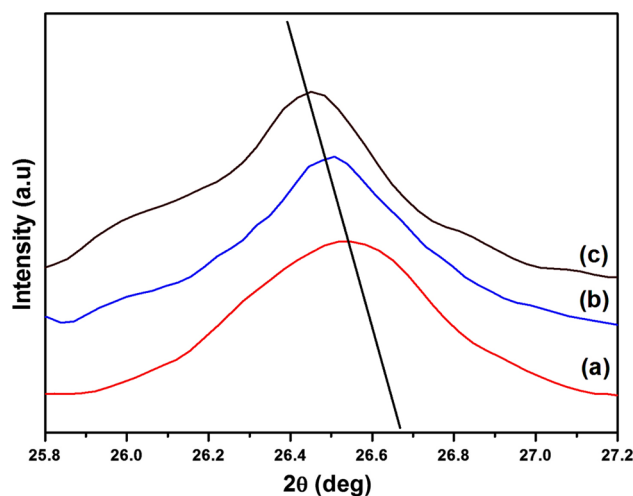


Fig. 2 X-ray diffraction pattern of $\text{Cd}_{1-x}\text{Ni}_x\text{S}$ thinfilms obtained at various Ni concentrations

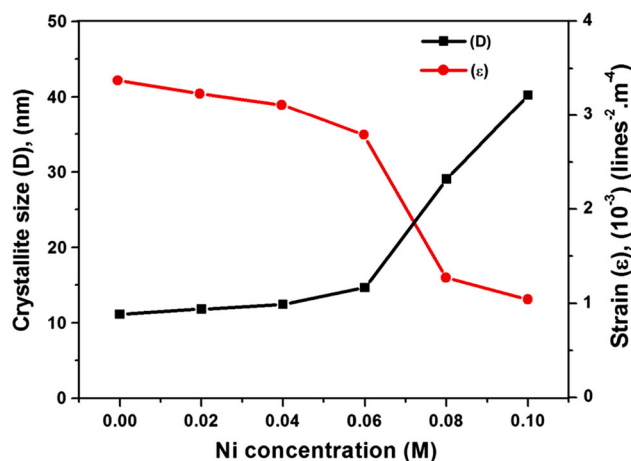


Fig. 3 The Crystallite size and strain values for $\text{Cd}_{1-x}\text{Ni}_x\text{S}$ thinfilms ($x = 0$ to 0.1 M)

$$D = \frac{k\lambda}{\beta \cos\theta}$$

Where λ is the wavelength of X-rays, θ is the Bragg diffraction angle, β is the FWHM of the XRD peak corresponding to the Bragg diffraction angle 2θ and D is the crystallite size. The strain (ϵ) was calculated using the relation.

$$\epsilon = \frac{\beta \cos\theta}{4}$$

Figure 3 shows the variation of crystallite size (D) and strain (ϵ) values of undoped and Ni doped CdS thinfilms with respect to Ni concentration. The crystallite size gradually increased from 11 to 40 nm with the increased Ni concentration. The strain gradually decreased with increase

Table 1 A summary of lattice constant, crystallite size, strain and bandgap values for varying Ni content

Ni concentration (X)	Interplanar distance (d) (Å)		Lattice constant (a) (Å)	Crystallite size (D) (nm)	Strain (ϵ)	Bandgap E_g (eV)
	Observed value	Calculated value				
0	3.3658	3.3668	5.8299	11.13	3.37	2.62
0.02	3.3638	3.3642	5.8239	11.82	3.21	2.60
0.04	3.3611	3.3627	5.8243	12.44	3.23	2.50
0.06	3.3608	3.3610	5.8217	14.66	3.09	2.41
0.08	3.3586	3.3592	5.8138	29.06	1.27	2.32
0.1	3.3572	3.3558	5.8139	40.23	1.04	2.28

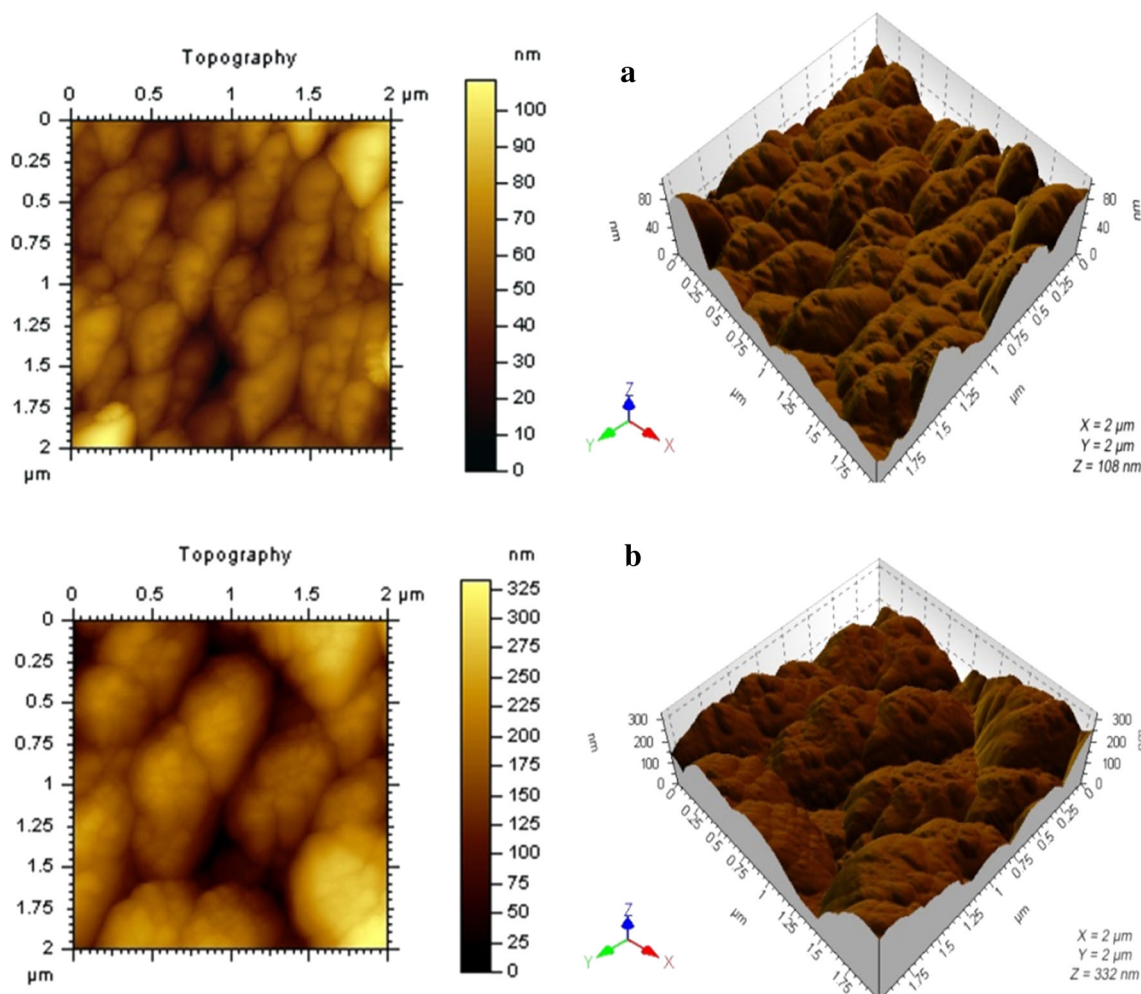


Fig. 4 Two-dimensional and Three-dimensional AFM images for $Cd_{1-x}Ni_xS$ thinfilms obtained at various Ni concentrations **a** $X = 0.06$ **b** $X = 0.08$ M

Fig. 5 SEM images for $\text{Cd}_{1-x}\text{Ni}_x\text{S}$ thinfilms obtained at various Ni concentrations **a** $X = 0$ **b** $X = 0.04$, **c** $X = 0.08$ and **d** EDAX for $X = 0.04$ M

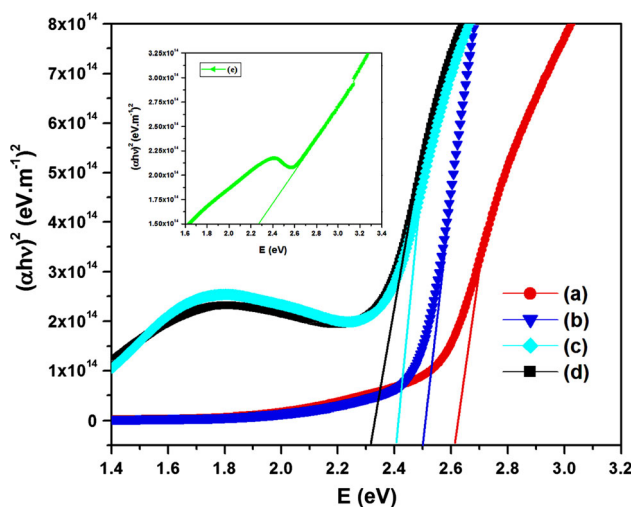
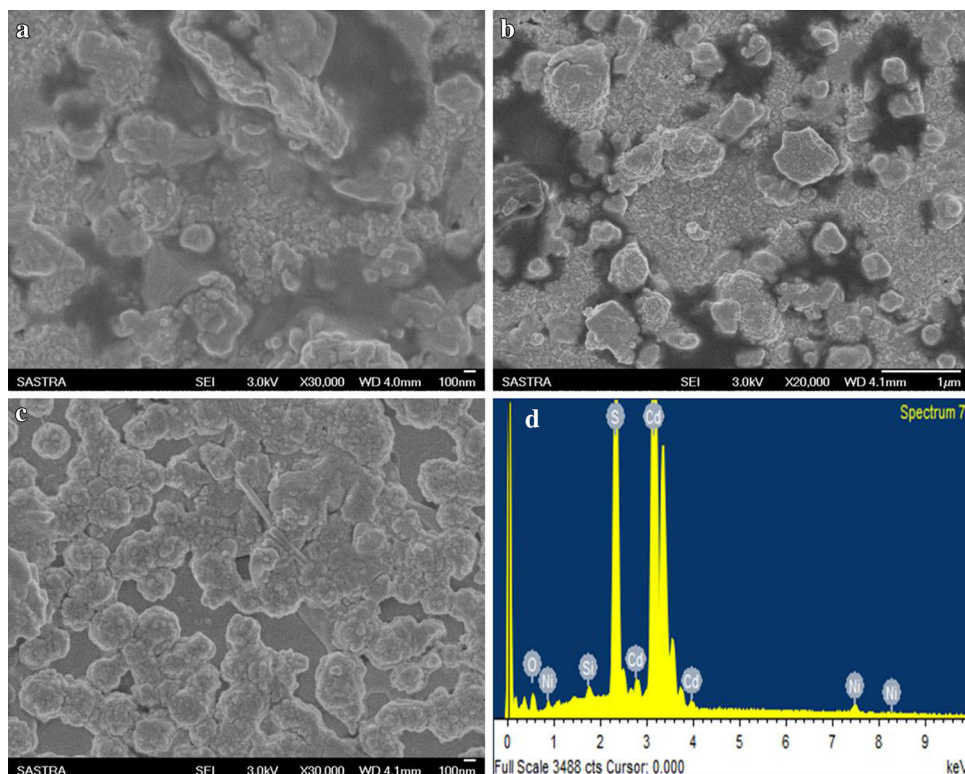


Fig. 6 Bandgap for $\text{Cd}_{1-x}\text{Ni}_x\text{S}$ thinfilms obtained at various Ni concentrations **a** $X = 0$ **b** $X = 0.04$ **c** $X = 0.06$ **d** $X = 0.08$ and **e** $X = 0.1$ M

of Ni content up to $X = 0.06$ M and then suddenly decreased with increased Ni content for $X = 0.08$ and 0.1 M. It is clear from the figure that the strain values decreased due to the increased crystallite sizes [14]. Summary of the structural results are presented in Table 1.

Figure 4a, b shows the atomic microscopy images of Ni doped CdS thinfilms at $x = 0.06$ and 0.08 M. The smaller grains are agglomerate together to form larger grains at

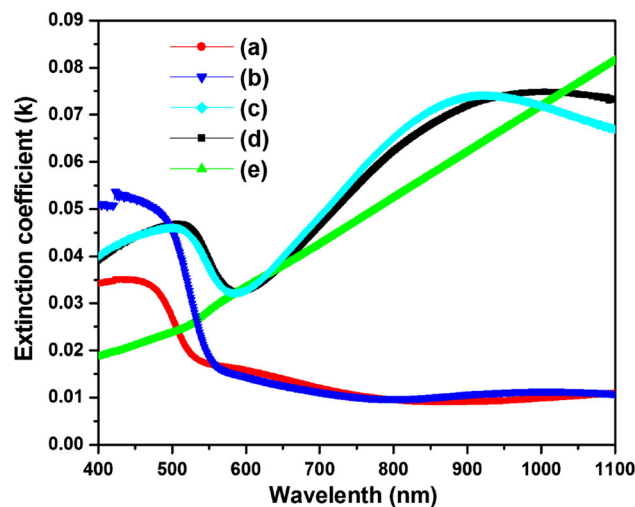


Fig. 7 Extinction coefficient for $\text{Cd}_{1-x}\text{Ni}_x\text{S}$ thinfilms obtained at various Ni concentrations **a** $X = 0$ **b** $X = 0.04$ **c** $X = 0.06$ **d** $X = 0.08$ and **e** $X = 0.1$ M

$x = 0.06$ M Ni concentrations. For Ni concentration at $x = 0.08$ M, the size of each grains differs from each other which indicating irregular growth rate of the grains. Grain sizes of the films are increased with increased Ni concentration and also increased the surface roughness of the films.

Scanning Electron Microscopy (SEM) pictures of pure CdS and Ni doped CdS films are shown in Fig. 5. From

Fig. 5a, there is no well-defined grain boundary with uneven shaped grains were observed. The small sized particles but agglomerated spherical like particles were observed in the Fig. 5b SEM images. The increased grain sized particles is revealed from the micrographs. Ni doped Cd_{1-x}Ni_xS (X = 0.08) films formed with homogeneity than the other undoped and Ni doped films. The bigger sizes of micro ranged particles are observed from Fig. 5c SEM picture. It may be due to agglomeration of nano particles and surface roughness increased with increased Ni concentrations. Figure 5d represents the Energy Dispersive Analysis X-ray spectra obtained Ni doped Cd_{1-x}Ni_xS (X = 0.04) films for composition analysis. The observed

peak of Cd, Ni and S confirms the presence of Ni doped CdS thin films.

The optical transmission spectra of the thin films were studied in the wavelength range of 400–1100 nm. The optical absorption coefficient (α) and bandgap (E_g) are related by [15]

$$\alpha h\nu = A(h\nu - E_g)^n$$

Where A is a constant and E_g is the bandgap of the materials and exponent n depends upon the type of transition. For direct transition $n = 1/2$, indirect transition $n = 2$. X = 0.02 Ni doped CdS and pure CdS films have very closed bandgap values because X = 0.02 have not any structural changes in the CdS structure but decrement in the band gap for increasing the dopant concentration is

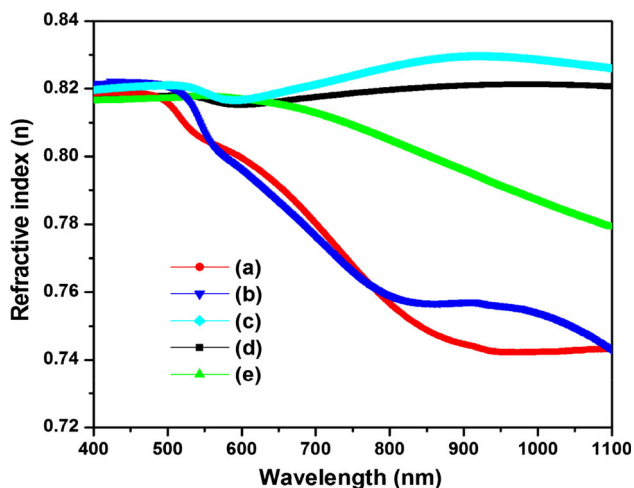


Fig. 8 Refractive index for Cd_{1-x}Ni_xS thinfilms obtained at various Ni concentrations a X = 0 b X = 0.04 c X = 0.06 d X = 0.08 and e X = 0.1 M

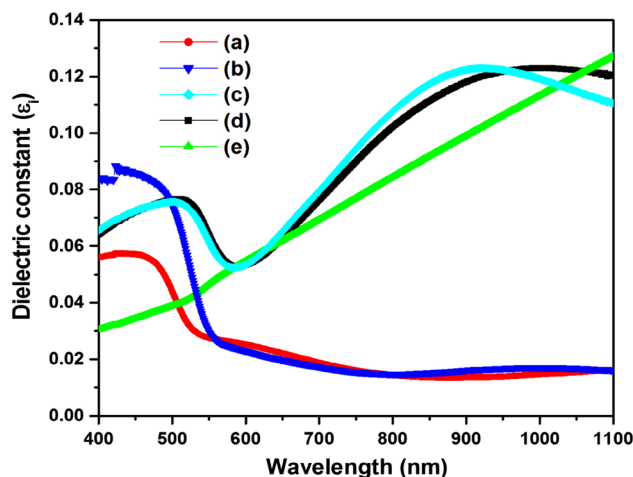


Fig. 10 Imaginary Part of Dielectric constant for Cd_{1-x}Ni_xS thinfilms obtained at various Ni concentrations a X = 0 b X = 0.04 c X = 0.06 d X = 0.08 and e X = 0.1 M

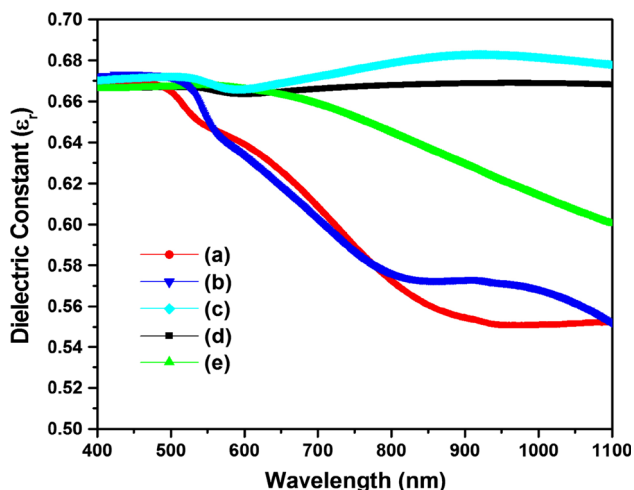


Fig. 9 Real Part of Dielectric constant for Cd_{1-x}Ni_xS thinfilms obtained at various Ni concentrations a X = 0 b X = 0.04 c X = 0.06 d X = 0.08 and e X = 0.1 M

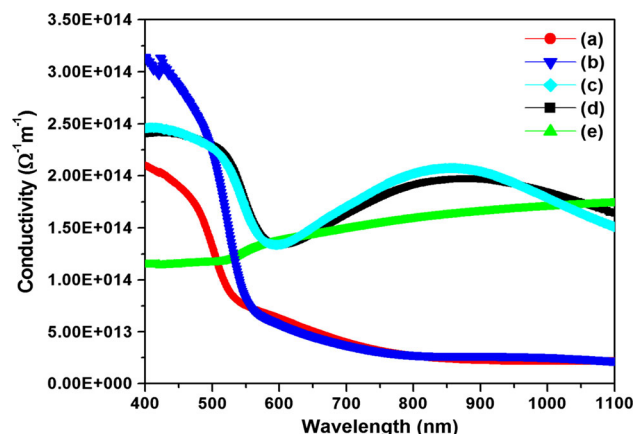
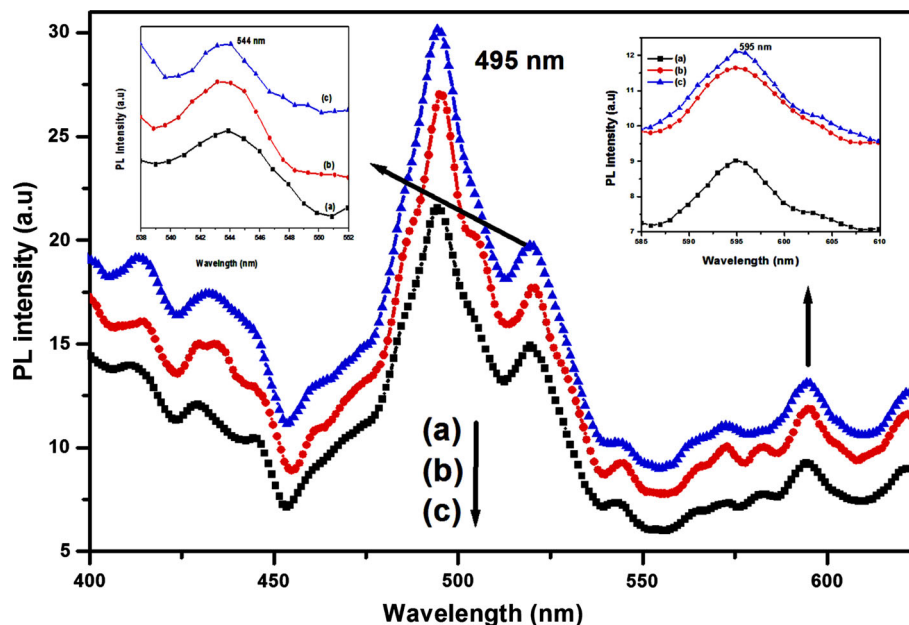


Fig. 11 Refractive index for Cd_{1-x}Ni_xS thinfilms obtained at various Ni concentrations a X = 0 b X = 0.04 c X = 0.06 d X = 0.08 and e X = 0.1 M

Fig. 12 Photoluminescence spectra of $\text{Cd}_{1-x}\text{Ni}_x\text{S}$ thinfilms obtained for **a** $X = 0.0$, **b** $X = 0.06$, **c** $X = 0.08$ M



the cause of incorporation of Ni^{2+} ions into the host which have 3d interaction with the valence electrons (sp) of CdS. The values of the extinction coefficient (k) of CdS thinfilms decreased with Ni concentration (Figs. 6, 7, 8 and 9 respectively). Similarly refractive index (n) of CdS thinfilms increases with Ni concentration. This is because as the Ni concentration increased with increased absorption coefficient.

However, change in refractive index due to change in Ni accounts with the crystallite sizes and internal strain with the films [16, 17]. The increase of refractive index with film thickness (t) shown in Figs. 10 and 11 respectively may be recognized as the increase of crystallite size with the decreases in microstrain.

The Photoluminescence (PL) spectra of the undoped and Ni doped CdS nanoparticles are shown in the Fig. 12. PL spectra consist many emission peaks indicates particle size distribution in the films. The PL spectrum of $\text{Cd}_{1-x}\text{Ni}_x\text{S}$ ($X = 0, 0.06$ and 0.08 M) thinfilms shows sharp emission peak at 490 nm with two right side shoulders at 545 and 595 nm. Here emission at 490 nm is the band edge emission due to the recombination of the exciton in the delocalized states of the films and it determines crystalline nature of nanoparticles [18, 19]. The peak at 545 nm is usually attributed to trap state emission arise from surface state defects. Commonly CdS films consists of Cd vacancies or S vacancies, interstitial of S and surface adsorption of Cd or S atoms.

Figure 13, shows the variation of magnetization as a function of magnetic field for Ni doped CdS films. The saturation magnetization (M_s) strongly depends on the dopant concentration of the films. The increase in M_s was probably caused by increase in electrons which induced more efficient

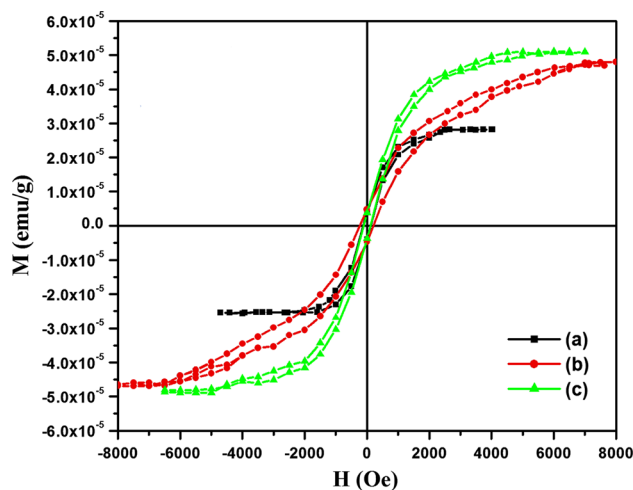


Fig. 13 VSM images for $\text{Cd}_{1-x}\text{Ni}_x\text{S}$ thinfilms obtained at various Ni concentrations **a** $X = 0.06$ **b** $X = 0.08$ and **c** $X = 0.1$ M

Table 2 Magnetic saturation, retention and coercivity values for Ni doped CdS thin films

Ni concentrations (X)	Magnetic saturation (M_s) ($\times 10^{-6}$) (emu)	Magnetic retentivity (M_R) ($\times 10^{-6}$) (emu)	Magnetic coercivity (H_C) (Oe)
0.06	26.31	3.69	104.78
0.08	45.62	3.74	138.31
0.1	51.34	3.77	104.73

ferromagnetic couplings between doped Ni^{2+} ions [20]. The free carrier concentrations are induced in Ni doped CdS films by the substitution of guest ions (Ni) into the host lattice (CdS)

will lead to room temperature ferromagnetism in the thinfilms [21]. The magnetic properties were tabulated in Table 2. The $\text{Cd}_{1-x}\text{Ni}_x\text{S}$ ($X = 0.4$) films shows less coercive value than $\text{Cd}_{1-x}\text{Ni}_x\text{S}$ ($X = 0.8$) films because of low concentrations of Ni content which dominated the sp-d electrons exchange interactions between sp electrons of CdS and d electrons of Ni^{2+} [22, 23]. The results are consistent with those of Ni doped CdS thin films prepared by chemical spray pyrolysis by Rmili et al. [24] and they have reported that superior thin films of Ni doped CdS with 4 % Ni can be grown by chemical spray method. The room temperature ferromagnetism has been reported for nanoparticles of CdS doped with Sanjeev Kumar et al. [25] for 3 % Ni doping and 3 % Ni, Cu co-doping. These studies revealed that chemical methods are suitable to produce DMS materials with ferromagnetic properties.

4 Conclusion

Undoped and Ni doped CdS thin films were deposited onto non conducting glass substrate using chemical bath deposition technique. The lattice structure of CdS films increased and also which starts to changes from cubic to hexagonal phase with the increased Ni concentrations. AFM images show the agglomeration of smaller to bigger grains by increasing Ni dopant in CdS thin films. The bandgap vales decreased from 2.62 to 2.28 eV by increased Ni content in the CdS structure. Simirally the magnetization is increased by induced ferromagnetic couplings between doped Ni^{2+} ions.

Acknowledgments The author has gratefully acknowledged the UGC- No. F.41-913/2012 (SR), India for providing financial support to carry out this work.

References

1. P. Zhang, P.S. Kim, T.K. Sham, *J. Appl. Phys.* **91**, 6038 (2002)
2. Y. Li et al., *J. Mater. Chem.* **15**, 917 (2005)

3. H. Liang, T.E. Angelini, P.V. Braun, G.C.L. Wong, *J. Am. Chem. Soc.* **126**, 14157 (2006)
4. H. Pan, J.B. Yi, L. Shen, R.Q. Wu, J.H. Yang, Y.P. Feng, J. Ding, L.H. Van, J.H. Yin, *Phys. Rev. Lett.* **99**, 127201 (2009)
5. Brus Le, *Appl. Phys. Lett.* **53**, 465 (1991)
6. R. Tenne, VM. Nabutovsky, E. Lifshitz, AF. Francis. *Solid State Commun.* **82**, 651 (1992)
7. I.O. Oladeji, L. Chow, *Thin Solid Films* **474**, 77 (2005)
8. N.V. Hullavarad, S.S. Hullavarad, P.C. Karulkar, *J. Nano Sci. Nano Technol.* **8**, 3272 (2008)
9. K. Gurumurugan, D. Mangalraj, Sa. K. Naratanadass. *J. Cryst. Growth* **147**, 355 (1995)
10. R.K. Gupta, K. Ghosh, R. Patel, S.R. Mishra, P.K. Kahol, *Mater. Lett.* **62**, 4103 (2008)
11. R. Ferro, J.A. Rodriguez, *Thin Solid Films* **347**, 295 (1999)
12. A.J. Varkey, A.F. Fort, *Thin Solid Films* **239**, 211 (1994)
13. E. Cetinorgu, C. Gumus, R. Esen, *Thin Solid Films* **2**, 1688 (2006)
14. A.L. Dawer, P.K. Shishodia, J. Chouhan, G. Kumar, A. Mathur, *Mater. Sci. Lett.* **9**, 547 (1990)
15. P. Sharma, V. Sharma, S.C. Katyal, *Cholcogenide Lett.* **3**, 73 (2006)
16. F. Tephany, N. Ozer, *Sol. Energy Mater. Sol. Cells* **30**, 353 (1993)
17. A. Ashour, N. El-Kdry, S.A. Mahmood, *Thin Solid Films* **269**, 117 (1995)
18. R.J. Heath, J.J. Shiang, *Chem. Soc. Rev.* **27**, 65 (1998)
19. M. Thambidurai, N. Muthukumarasamy, S. Agilan, N. Murugan, S. Vasantha, R. Balasundaraprabhu, T.S. Senthil, *J. Mater. Sci.* **45**, 3254 (2010)
20. X.C. Liu, E.W. Shi, Z.Z. Chen, H.W. Zhang, B. Xiao, L.X. Song, *Appl. Phys. Lett.* **88**, 252503 (2006)
21. D. Chakraborti, S. Ramachandran, Trichy G. Narayan and JT. Prater. *J. Appl. Phys.* **101**, 053918 (2007)
22. M. Elango, K. Gopalakrishnan, S. Vairam, M. Tamilselvam, *J. Alloys Compd.* **538**, 48 (2012)
23. P. Venkatesu, K. Ravichandran, *Adv. Mat. Lett.* **4**, 202 (2013)
24. A. Rmili, F. Ouachtar, A. Bouaoud, A. Louardi, T. Chtouki, B. Elidrissi, H. Erguig, *J. Alloys Compd.* **557**, 53 (2013)
25. S. Kumar, S. Kumar, S. Jain, N.K. Verma, *Appl. Nanosci* **2**, 127–131 (2012)